AAC Journals.ASM.org

Heteroresistance to Fosfomycin Is Predominant in *Streptococcus pneumoniae* and Depends on the *murA1* Gene

Hansjürg Engel,[a,b] Javier Gutiérrez-Fernández,[c] Christine Flückiger,[a] Martín Martínez-Ripoll,[c] Kathrin Mühlemann,[a,d]† Juan A. Hermoso,[c] Markus Hilty,[a,d] Lucy J. Hathaway[a]

Institute for Infectious Diseases, Faculty of Medicine, University of Bern, Bern, Switzerland[a]; Graduate School for Cellular and Biomedical Sciences, University of Bern, Bern, Switzerland[b]; Department of Crystallography and Structural Biology, Instituto de Química-Física Rocasolano, CSIC, Madrid, Spain[c]; Department of Infectious Diseases, University Hospital, Bern, Switzerland[d]

Fosfomycin targets the first step of peptidoglycan biosynthesis in *Streptococcus pneumoniae* catalyzed by UDP-*N*-acetylglucosamine enolpyruvyltransferase (MurA1). We investigated whether heteroresistance to fosfomycin occurs in *S. pneumoniae*. We found that of 11 strains tested, all but 1 (Hungary^{19A}) displayed heteroresistance and that deletion of *murA1* abolished heteroresistance. Hungary^{19A} differs from the other strains by a single amino acid substitution in MurA1 ($Ala_{364}Thr$). To test whether this substitution is responsible for the lack of heteroresistance, it was introduced into strain D39. The heteroresistance phenotype of strain D39 was not changed. Furthermore, no relevant structural differences between the MurA1 crystal structures of heteroresistant strain D39 and nonheteroresistant strain Hungary^{19A} were found. Our results reveal that heteroresistance to fosfomycin is the predominant phenotype of *S. pneumoniae* and that MurA1 is required for heteroresistance to fosfomycin but is not the only factor involved. The findings provide a caveat for any future use of fosfomycin in the treatment of pneumococcal infections.

Pneumococci have responded to antimicrobial treatment by acquiring resistance to antibiotics, particularly penicillin (1). However, although knowledge of classical resistance mechanisms is increasing (2, 3), understanding of the penicillin heteroresistance phenomenon described in pneumococci remains elusive (4).

Heteroresistance is the ability of a clonal population to grow one or several subpopulations at a frequency of 10^{-7} to 10^{-3} in the presence of a higher antibiotic concentration than that predicted to be effective by measurement of the MIC (4). This phenomenon may allow some bacteria to grow at higher antibiotic concentrations without the fitness cost required by a genetically fixed resistance mechanism. Furthermore, heteroresistance allows some bacteria to survive antimicrobial treatment while at the same time making conventional resistance testing unreliable (4, 5). Heteroresistance to different antibiotics has been described in pathogens of various species (6–9), but even for the most extensively studied (heteroresistance to methicillin, oxacillin, and vancomycin in staphylococci [10–16]), the mechanism is unknown. Understanding heterogeneity between single cells is complicated by the fact that conventional assays of microbial populations consider an averaged value of thousands or millions of cells in a sample (17).

Fosfomycin (18) is not currently used in the treatment of pneumococcal infections, but in this era of multidrug resistance, studies of this antibiotic may be valuable to inform decisions on future antibiotic use (19). Fosfomycin is a drug of particular interest for its synergy with benzylpenicillin, by decreasing the production of penicillin-binding proteins. This is beneficial in the treatment of infections with β-lactam-resistant pneumococci (20). Combinations of other antibiotics with fosfomycin are used successfully in the treatment of infections with other organisms, such as *Staphylococcus aureus* (21). The target of fosfomycin is MurA (UDP-*N*-acetylglucosamine enolpyruvyltransferase, EC 2.5.1.7), an enzyme catalyzing the first step of the peptidoglycan biosynthetic pathway of Gram-positive and Gram-negative microorganisms. MurA transfers the enolpyruvyl group of phosphoenolpyruvate (PEP) to UDP-*N*-acetylglucosamine (UDP-GlcNAc), producing enolpyruvyl UDP-*N*-acetylglucosamine (EP-UDP-GlcNAc) (22, 23). Gram-positive bacteria have two genes, *murA1* and *murA2*, both encoding active MurA enzymes with similar catalytic parameters and conserved major structural features that are both inhibited by fosfomycin (24).

Mutagenesis experiments have revealed that fosfomycin covalently binds to Cys115 of MurA, suggesting that this amino acid plays an important role in the catalytic mechanism (25, 26). The Cys115 residue has been suggested to be the general acid catalyst, protonating C-3 of PEP prior to nucleophilic attack by UDP-GlcNAc to form the tetrahedral intermediate (27, 28), although other experiments indicate that a different amino acid (Asp) plays this role (29). Recent studies have shown that MurA forms dormant complexes with UDP-*N*-acetylmuramic acid (UDP-MurNAc), which is the product of MurB, the second enzyme partici-

Received 1 February 2013 **Returned for modification** 21 February 2013
Accepted 4 April 2013

Published ahead of print 9 April 2013

Address correspondence to Lucy J. Hathaway, lucy.hathaway@ifik.unibe.ch.

† Deceased 1 November 2012.

M.H. and L.J.H. contributed equally to this work.

We dedicate this work to the memory of Kathrin Mühlemann, who designed and guided research for this study, encouraging us to overcome difficulties of any kind. Her expertise and friendship are sorely missed.

Supplemental material for this article may be found at http://dx.doi.org/10.1128/AAC.00223-13.

doi:10.1128/AAC.00223-13

TABLE 1 Frequency of subpopulations with higher fosfomycin and penicillin resistance levels in selected *S. pneumoniae* strains

Strain	MLST type	Serotype	Fosfomycin MIC (μg/ml)[a]	Frequency of cells with higher fosfomycin resistance[b]	Penicillin MIC (μg/ml)[c]	Frequency of cells with higher penicillin resistance[c]	Reference or source
Wild types							
207.41	179	19F	32	10^{-4}–10^{-5}	0.064	0	48
208.39	276	19F	3.0	10^{-4}–10^{-5}	0.75	10^{-3}–10^{-5}	4
304.80	179	19F	3.0	10^{-2}–10^{-5}	0.75	10^{-3}–10^{-5}	48
106.44	344	nt	8.0	10^{-5}–10^{-6}	1.0	10^{-4}–10^{-5}	49
110.58	344	nt	8.0	10^{-3}–10^{-5}	0.19	10^{-6}	49
Spain^{9V}-3	156	9V	24	10^{-4}	2.0	10^{-3}–10^{-6}	ATCC 700671
Hungary^{19A}-6	268	19A	6.0	0	1.0	10^{-3}–10^{-5}	ATCC 700673
Finland^{6B}-12	270	6B	3.0	10^{-3}–10^{-6}	0.38	10^{-3}	ATCC 700903
Taiwan^{23F}-15	242	23F	12	10^{-6}	1.5	10^{-3}–10^{-6}	ATCC 700906
South Africa^{19A}-7	75	19A	12	10^{-4}–10^{-6}	0.38	0	ATCC 700674
D39	128	2	16	10^{-5}–10^{-6}	0.023	0	50
Δ*murA1* mutants							
106.44Δ*murA1*	344	nt	1.5	0	0.5	10^{-5}–10^{-6}	This study
Taiwan^{23F}Δ*murA1*	242	23F	1.5	0	0.5	10^{-2}–10^{-5}	This study
D39Δ*murA1*	128	2	2.0	0	0.016	0	This study
Hungary^{19A}Δ*murA1*	268	19A	2.0	0	0.5	10^{-3}–10^{-5}	This study
Switch mutants							
D39::$murA1_{Hungary}$	128	2	16.0	10^{-5}–10^{-6}	0.032	0	This study
Hungary::$murA1_{D39}$	268	19A	8.0	0	0.5	10^{-4}–10^{-6}	This study
D39::$murA1+murB_{Hungary}$	128	2	16.0	10^{-5}–10^{-6}	0.016	ND[d]	This study
Hungary::$murA1+murB_{D39}$	ND	19A	8.0	0	0.75	ND[d]	This study
Back transformants							
D39::$murA1_{D39}$	128	2	16.0	10^{-5}–10^{-6}	0.016	0	This study
Hungary::$murA1_{Hungary}$	268	19A	8.0	0	0.75	10^{-3}–10^{-5}	This study

[a] MIC determined by Etest.
[b] Frequency of subpopulations with higher fosfomycin resistance levels as determined by PAP (4).
[c] Values for wild types as reported by Morand and Mühlemann (4).
[d] ND, not determined.

pating in peptidoglycan synthesis. This supports the idea that Cys115 provides tight product regulation and protection, which are absent from species containing aspartic acid in this position (30).

At the structural level, MurA can exist in open and closed conformations (31, 32). Native enzymes are in the open conformation and then close when UDP-GlcNAc enters the catalytic pocket. This closure consists of the movement of the loop containing Cys115 over UDP-GlcNAc, creating the optimal environment for the addition-elimination reaction.

After describing heteroresistance to penicillin in *Streptococcus pneumoniae* (4), we investigated whether the heteroresistance phenomenon also exists in an early step of peptidoglycan biosynthesis. Therefore, we tested a representative selection of pneumococcal strains for heteroresistance to fosfomycin, which acts earlier in the peptidoglycan synthesis pathway than penicillin. Here we report for the first time that heteroresistance to fosfomycin occurs in *S. pneumoniae* and investigate the role of MurA1 in this phenotype.

MATERIALS AND METHODS

Bacterial strains. Eleven strains including five clinical isolates of *S. pneumoniae* from two nationwide surveillance programs collecting nasopharyngeal and invasive isolates, five international reference strains, and laboratory strain D39, all listed in Table 1, were used for this study.

Construction of mutants. For the construction of *murA1* knockout mutants, *murA1* was disrupted with the bicistronic cassette Janus (33). Transformation of strains 106.44, Taiwan^{23F}, Hungary^{19A}, and D39 was performed as described elsewhere (34). Insertion of the cassette was confirmed by PCR. Mutant Hungary::$murA1_{D39}$ and D39::$murA1_{D39}$ back transformants were obtained by the insertion of a construct with $murA1_{D39}$ fused to a spectinomycin resistance cassette to allow selection as described previously (35). Mutant D39::$murA1_{Hungary19A}$ and Hungary::$murA1_{Hungary19A}$ back transformants were obtained after the insertion of the $murA1_{Hungary19A}$-spectinomycin resistance cassette construct, which was created by the introduction of mutation $G_{1090}A$ into the $murA1_{D39}$-spectinomycin resistance cassette construct. Switch mutants of *murB*, i.e., Hungary::$murA1+murB_{D39}$ and D39::$murA1+murB_{Hungary19A}$, were obtained by the introduction of a construct with $murB_{D39}$ or $murB_{Hungary19A}$, respectively, fused to a kanamycin resistance cassette into *murA1* switch mutants. The *murA1* and *murB* sequences of all switch mutants and back transformants were confirmed as described before (36). For more details about the procedures used, see Materials and Methods in the supplemental material.

Susceptibility testing and PAP. Fosfomycin MICs were determined by the Etest method (bioMérieux, Geneva, Switzerland) according to the manufacturer's protocol. Population analysis profiles (PAPs) were prepared as described earlier (4). Briefly, bacteria were cultured to mid-log phase (optical density at 600 nm [OD_{600}] of 0.7) and dilutions of 10^{-2} to 10^{-4} and 10^{-6} in phosphate-buffered saline (pH 7.4) were prepared. A 100-μl volume was

plated on Müller-Hinton broth plates with 5% sheep blood containing fosfomycin (fosfomycin disodium; Chemical Abstracts Service no. 26016-99-9) in concentrations ranging from 0 to 500 μg/ml. Colonies were counted by eye after 48 h of incubation at 37°C in 5% CO_2.

Gene expression studies. Bacteria were grown overnight in 5% brain heart infusion broth (BHI)–fetal calf serum (FCS) for 9 h at 37°C, and then 200 μl of the overnight culture was rediluted in 20 ml of BHI-FCS and grown to an OD_{600} 0.6. A 20-ml volume of RNAprotect (Qiagen) was then added, RNA was extracted, and the expression of *murA1* and *murA2* was quantified by real-time reverse transcription (RT)-PCR as described elsewhere (37). For the primers and probes used, see Table S1 in the supplemental material. Quantification of *murA1* and *murA2* expression in wild-type strains was done four times, and quantification of *murA2* expression in Δ*murA1* mutant strains was measured in triplicate.

Recombinant protein expression. The *murA1* sequences of strains D39 and Hungary^{19A} were cloned into pGEX-6p-1 and expressed in *Escherichia coli* BL21 cells. Purification of recombinant protein was performed by glutathione Sepharose 4 Fast Flow chromatography (GE Healthcare, Stockholm, Sweden) as suggested by the manufacturer. Protein samples were analyzed by SDS-PAGE and were >95% of the expected protein. Identities of recombinant proteins were confirmed by mass spectrometric peptide fingerprinting. For more details, see Materials and Methods in the supplemental material.

MurA1$_{D39}$ and MurA1$_{Hungary19A}$ crystallization and data collection and processing. Crystallization conditions were screened (PACT Suite and JCSG Suite from Qiagen, Hilden, Germany; JBScreen Classic 1-4 from Jena Bioscience, Jena, Germany; Crystal Screen, Crystal Screen 2, and Index HT from Hampton Research) by high-throughput techniques with a NanoDrop robot and Innovadyne SD-2 microplates (Innovadyne Technologies Inc.). Conditions were optimized by a hanging-drop vapor diffusion method, mixing of 1 μl of protein solution and 1 μl of precipitant solution and equilibration against 500 μl of reservoir solution.

MurA1$_{D39}$ protein crystals were obtained in 50 mM $CaCl_2$–100 mM HEPES (pH 7.5)–24% (wt/vol) polyethylene glycol (PEG) 4000 at a concentration of 14 mg/ml. MurA1$_{Hungary19A}$ crystals were obtained in 0.2 M ammonium acetate–0.1 M sodium citrate tribasic dihydrate (pH 5.6)–30% (wt/vol) PEG 4000 at a concentration of 7.5 mg/ml. Crystals of both proteins were cryoprotected in 20% (vol/vol) glycerol before collection of diffraction data by the use of synchrotron radiation at beamline PX3 in the Swiss Light Source (SLS), Zurich, Switzerland. MurA1$_{D39}$ crystals diffracted up to 2.9 Å resolution and belonged to the $P2_12_12_1$ orthorhombic space group (a = 46.62 Å, b = 81.11 Å, c = 104.88 Å, α = β = γ = 90°). One single monomer was found in the asymmetric unit, yielding a Matthews coefficient (38) of 2.18 Å^3 Da^{-1} and a solvent content of 43.5%. MurA1$_{Hungary19A}$ crystals diffracted up to 1.8 Å resolution and belonged to the $P2_12_12$ orthorhombic space group (a = 106.58 Å, b = 70.36 Å, c = 45.24 Å, α = β = γ = 90°). One single monomer was found in the asymmetric unit, yielding a Matthews coefficient of 1.86 Å^3 Da^{-1} and a solvent content of 33.9%. Diffraction data sets were processed with XDS (39) and SCALA (40, 41).

MurA1$_{D39}$ and MurA1$_{Hungary19A}$ structural determination and refinement. MurA1$_{D39}$ and MurA1$_{Hungary19A}$ crystal structures were obtained by molecular replacement, which was performed with Phaser (42) by using MurA from *Enterobacter cloacae* (31) (Protein Data Bank [PDB] code 1NAW) as the initial model for the MurA1$_{Hungary19A}$ data set and then MurA1$_{Hungary19A}$ as the model for MurA1$_{D39}$. Refinement and model building of both structures were performed with Phenix (43) and Coot (44), respectively. The refinement converged to the final values of R_{work} = 0.16 and R_{free} = 0.20 for MurA1$_{D39}$ and R_{work} = 0.18 and R_{free} = 0.24 for MurA1$_{Hungary19A}$ (Table 2). Analysis of these models with MolProbity showed good stereochemistry (45). The quality of the electron density map allowed the modeling of MurA1$_{D39}$ from Met1 to Asp419, although some residues belonging to a flexible loop were not included in the final model (from Gly114 to Pro120). The modeling of MurA1$_{Hungary19A}$ involved residues Met1 to Glu418, although two regions were not included in the final models (from Pro113 to Cys116 and from Tyr85 to Lys87). All graphic representations were prepared with PyMOL.

TABLE 2 X-ray data collection and refinement statistics for MurA1$_{D39}$ and MurA1$_{Hungary19A}$

Parameter	Measurement[a]	
	MurA1$_{D39}$	MurA1$_{Hungary19A}$
Space group	$P2_12_12_1$	$P2_12_12$
a (Å)	46.62	106.58
b (Å)	81.11	70.36
c (Å)	104.88	45.24
α = β = γ (°)	90	90
Resolution range (Å)	44.0–2.9	45.2–1.8
Beamline	PX3 (SLS)	PX3 (SLS)
Wavelength (Å)	1	1
No. of reflections		
Total	185,839	420,364
Unique	14,373	32,258
R_{pim}[b]	0.114 (0.427)	0.039 (0.351)
Mean I/σ (I)	7.0 (1.9)	16.3 (2.3)
Completeness (%)	100	99.7
Redundancy	6.5 (6.2)	12.7 (13.0)
Refinement		
No. of atoms (non-H)	3,132	3,506
R_{work}/R_{free}[c]	0.18/0.24	0.16/0.20
RMS[d] bond deviations		
Length (Å)	0.002	0.007
Angle (°)	0.504	1.07
PDB code	3HZ3	3HZ4

[a] Values in parentheses are for the highest-resolution shell.
[b] $R_{pim} = \sum_{hkl}[1/(N-1)]^{1/2}\sum_i |I_i(hkl) - [I(hkl)]|/\sum_{hkl}\sum_i I_i(hkl)$, where $I_i(hkl)$ is the ith measurement of reflection hkl, $[I(hkl)]$ is the weighted mean of all measurements, and N is the redundancy of the hkl reflection.
[c] $R_{work}/R_{free} = \sum_{hkl}||F_o| - |F_c||/\sum_{hkl}|F_o|$, where F_c is the calculated and F_o is the observed structure factor amplitude of reflection hkl for the working/free (5%) set, respectively.
[d] RMS, root mean square.

Nucleotide sequence accession numbers. The atomic coordinates and structure factors for MurA1$_{D39}$ and MurA1$_{Hungary19A}$ have been deposited in the Protein Data Bank, Research Collaboratory for Structural Bioinformatics, Rutgers University (http://www.rcsb.org/), under codes 3ZH3 and 3ZH4, respectively. The GenBank accession numbers for MurA1 of D39 and Hungary^{19A} are YP_816443.1 and YP_001694508.1, respectively.

RESULTS AND DISCUSSION

Heteroresistance to fosfomycin was exhibited by the majority of the strains studied. Heteroresistance to penicillin has been described in *S. pneumoniae* and is hypothesized to be due to a combination of auxiliary genes acting in concert with one or more *pbp* genes, the products of which are inhibited by penicillin (4). Here we investigated whether we could observe heteroresistance to fosfomycin, an antibiotic acting on an earlier step of peptidoglycan biosynthesis than penicillin. Fosfomycin inhibits MurA1 and MurA2; enzymes that catalyze the first step of peptidoglycan biosynthesis. MurA1 and MurA2 have conserved major structural features and similar catalytic parame-

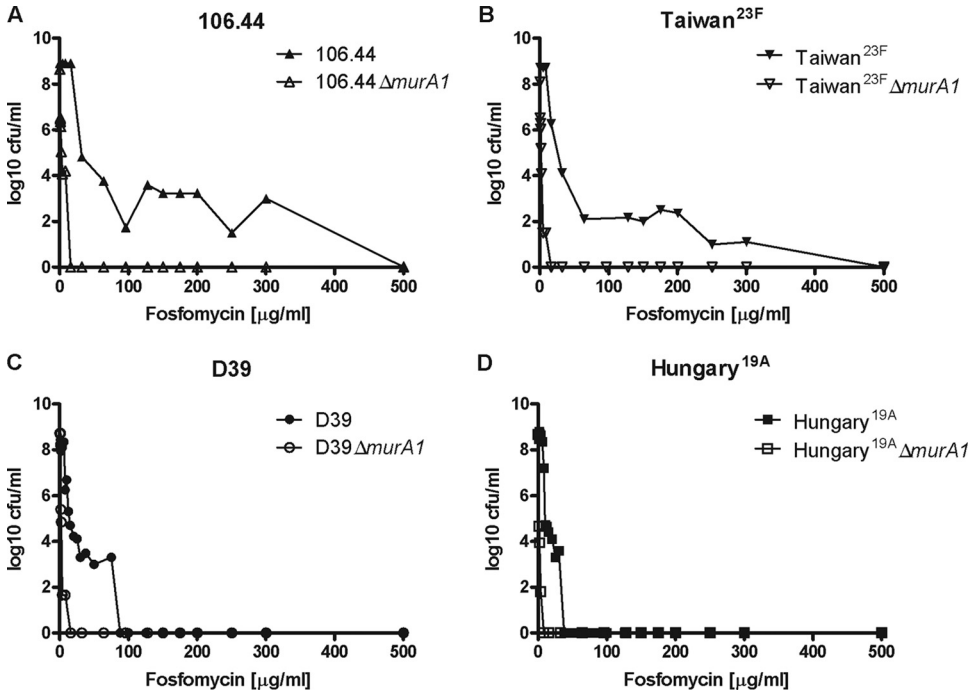

FIG 1 PAPs of *S. pneumoniae* wild-type and *murA1* knockout strains. An experiment representative of three independent experiments is shown. The concentration of fosfomycin used to select subpopulations with higher fosfomycin resistance levels is shown against the frequency of bacteria able to grow at that concentration. Wild-type and *murA1* knockout mutant forms of Swiss clinical strain 106.44 (A), international reference strain Taiwan^{23F} (B), laboratory strain D39 (C), and international reference strain Hungary^{19A} (D) are shown. A horizontal plateau in the curve, such as that shown for strain 106.44 in panel A, indicates heteroresistance, in contrast to a steep drop in the curve indicating no heteroresistance, as shown for strains Hungary^{19A} in panel D.

ters and are both inhibited by fosfomycin with comparable efficiency (24).

Within the 11 strains we tested, representing Swiss clinical strains, international reference strains and laboratory strains, we found that heteroresistance to fosfomycin was the predominant phenotype as all of the strains but one, Hungary^{19A}, were heteroresistant to fosfomycin (Table 1). Heteroresistance to penicillin, although the predominant phenotype, was exhibited by only 8 of the 11 strains. This suggests that different mechanisms cause the heterogeneous expression of resistance to penicillin and fosfomycin.

Fosfomycin is not currently used as a treatment for pneumococcal infections, so the predominance of the heteroresistance phenotype in the absence of selective pressure was unexpected. Still, the fosfomycin MICs determined all ranged from 3 to 32 μg/ml (Table 1), which reflects the usual distribution of fosfomycin MICs for pneumococci (http://mic.eucast.org/Eucast2/). However, growth of heteroresistant strains at up to 300 μg/ml fosfomycin was observed (Fig. 1), demonstrating the threat that heteroresistance could pose, although its clinical significance remains controversial (5).

As a differentiating element unique to Hungary^{19A}, we identified a mutation in *murA1*. Therefore, we investigated further the role of MurA1 in heteroresistance.

Deletion of *murA1* abolished heteroresistance. The influence of the fosfomycin target MurA1 on heteroresistance was analyzed by comparing the PAPs of wild-type and Δ*murA1* mutant strains. Knockout of *murA1* leads to abolishment of the heteroresistance phenotype (Fig. 1) and a drastic reduction of the fosfomycin MIC (Table 1) for all of the strains tested, indicating that it does indeed mediate heteroresistance to this antibiotic. However, heteroresistance to penicillin was conserved in the mutants, supporting the hypothesis that distinct mechanisms determine heteroresistance to penicillin and fosfomycin.

Expression of *murA1* and *murA2* did not differ between strains. To determine whether heteroresistance to fosfomycin in the wild-type strains is due to differences in the expression of the fosfomycin targets MurA1 and MurA2, expression was quantified by real-time RT-PCR (Fig. 2A and B).

There was no significant difference between strains in the expression of either *murA1* or *murA2*, indicating that MurA1/A2 expression levels do not determine heteroresistance. In addition, knocking out *murA1* did not result in a compensatory upregulation of *murA2* for any of the strains tested (Fig. 2C). A limitation of these experiments is that expression levels were measured in liquid culture in the absence of antibiotic and therefore may not represent the expression of MurA within a highly resistant subpopulation in a heteroresistant strain. Experiments conducted with colonies grown in different antibiotic concentrations (not shown) showed extremely variable MurA1 expression patterns, making the results difficult to interpret, which is why Fig. 2 represents the results of liquid culture in the absence of antibiotic.

An Ala$_{364}$Thr substitution in MurA1 did not influence heteroresistance. Sequencing of MurA1 revealed a mutation leading to an Ala$_{364}$Thr substitution in strain Hungary^{19A}. To determine whether this mutation confers a significant conformational change, we solved the three-dimensional structures of *S. pneu-*

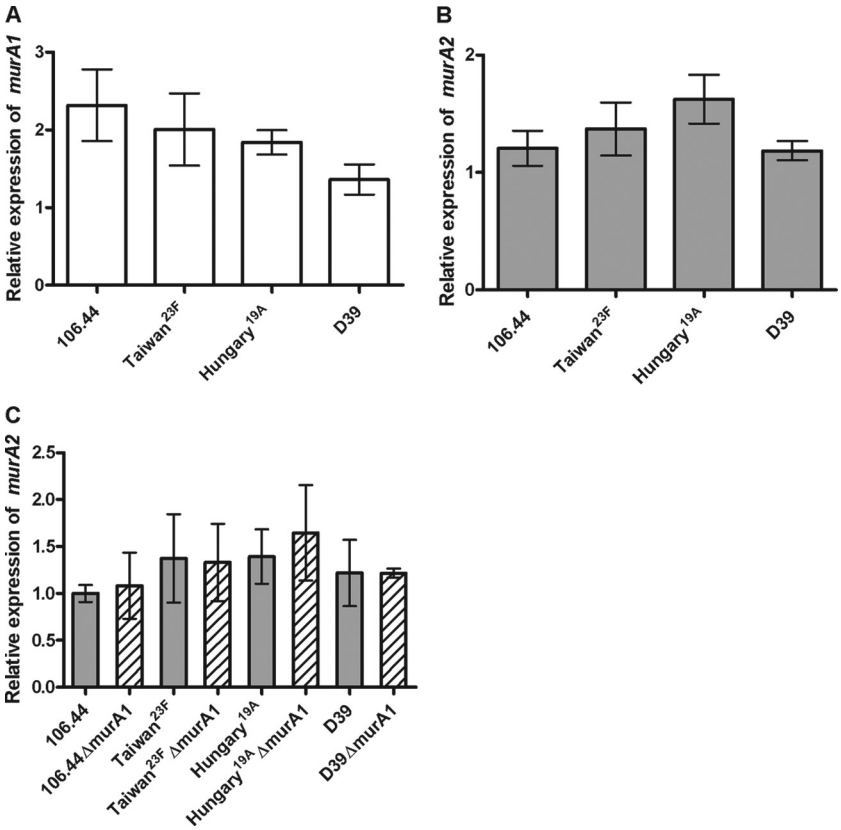

FIG 2 Relative levels of *murA1* (A) and *murA2* (B) expression in *S. pneumoniae* wild-type strains. (C) Comparison of *murA2* expression levels in wild-type (gray bars) and *murA1* knockout (hatched bars) strains. Expression is displayed as a value relative to that of the isolate with the lowest expression level after normalization to 16S RNA gene expression. Values are means of three independent experiments. The standard error of the mean is shown. No significant differences were detected by analysis of variance.

moniae $MurA1_{D39}$ and $MurA1_{Hungary19A}$ at 2.9 and 1.8 Å resolutions, respectively.

The *S. pneumoniae* MurA1 enzyme consists of a single chain of 419 residues forming two globular domains (I and II) linked by a double-stranded hinge (residues 19 to 20 and 231 to 233) (Fig. 3). The overall structure of this protein follows the folding previously described for the *E. cloacae* MurA enzyme (31). The closest structural homologue of $MurA1_{D39}$ is the open conformation of *E. cloacae* MurA (PDB code 1EJD), whereas for $MurA1_{Hungary19A}$ it is the closed conformation of *Bacillus anthracis* MurA (PDB code 3SG1) (see Fig. S1 in the supplemental material). The loop containing catalytic Cys116 (residues 110 to 122) presents some differences compared with that of close homologues (see Fig. S2). Most of this loop showed strong flexibility, in agreement with previous works in which this flexibility has been reported (31, 46).

The crystal structure of $MurA1_{D39}$ presents an open conformation (Fig. 3A), while $MurA1_{Hungary19A}$ showed a closed conformation; this is probably due to the unexpected action of the citrate buffer in the catalytic pocket. Citrate buffer was found attached to the active site occupying the position of PEP and fosfomycin (Fig. 3B). The difference between the open and closed conformations is an angle of about 20° between their domains.

The only difference between $MurA1_{D39}$ and $MurA1_{Hungary19A}$ concerns the $Ala_{364}Thr$ substitution. This mutation is located 25 Å away from the active site in domain I (Fig. 3). Structural inspection of this region reveals no significant changes in the main chain (root mean square deviation of 0.546 Å for the Cα atoms of domain I) or in the amino acid interaction networks that could propagate to the active site affecting catalytic activity (Fig. 3C). This structural similarity between $MurA1_{D39}$ and $MurA1_{Hungary19A}$ suggests that the $Ala_{364}Thr$ substitution is not involved in the heteroresistance phenomenon. Notwithstanding the absence of significant conformation alteration by the mutation, the influence of the amino acid substitution on a differential dynamic contribution between the two proteins cannot be discounted, as has been described previously for a variant of the TEM-1 β-lactamase of *E. coli* (47).

The findings of the structural analysis are confirmed by the assessment of *murA1* switch mutants in PAPs. Compared to the wild-type strains (Fig. 4A), transfer of $murA1_{Hungary19A}$ did not lead to abolishment of the heteroresistance phenotype in D39, clearly distinguishable by the plateau in the PAP curve representing the growth of colonies over a fosfomycin concentration range of 12.5 to 75 μg/ml, nor did heteroresistance appear upon the insertion of $murA1_{D39}$ into the $Hungary^{19A}$ background (Fig. 4B). The spectinomycin resistance cassette used for the selection of the mutants created did not influence the heteroresistance phenotype, as demonstrated by the comparison of back transformants with the wild-type strains (Fig. 4C).

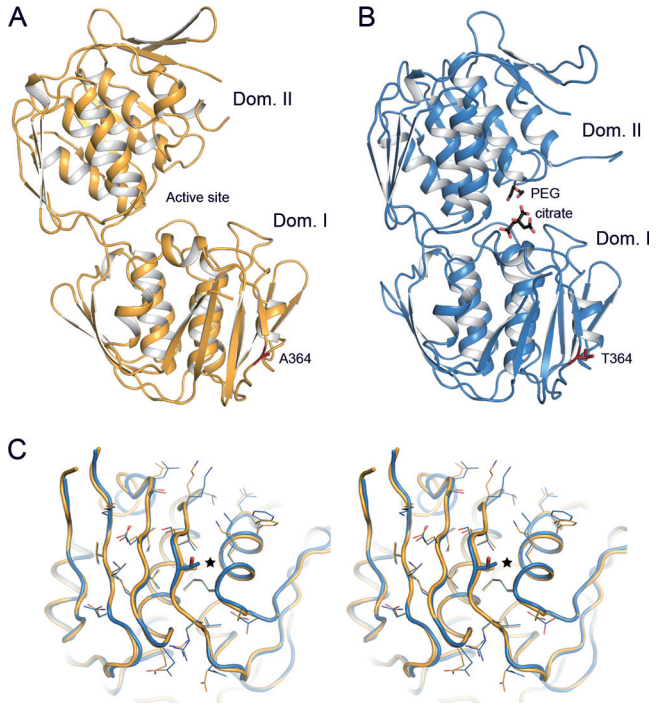

FIG 3 Crystal structure of pneumococcal MurA1. (A) Overall structure of *S. pneumoniae* $MurA1_{D39}$ in an open conformation. Ala_{364} is represented as capped sticks and colored red. (B) Overall structure of *S. pneumoniae* $MurA1_{Hungary19A}$ in a closed conformation, showing a citrate and a PEG molecule in the catalytic pocket (black-capped sticks). Thr_{364} is represented as capped sticks and colored red. (C) Stereo view of the superposition of domain I of $MurA1_{D39}$ (orange) and $MurA1_{Hungary19A}$ (blue). The Ala_{364}Thr mutation is represented in sticks and highlighted (star). Side chains of residues around position 364 are drawn as lines to show that there are no relevant modifications upon mutation. Dom., domain.

A previous study reported that the product of the MurB enzyme UDP-MurNAc of *E. cloacae* binds tightly to MurA, creating a dormant complex. Therefore, UDP-MurNAc could act as a negative feedback regulator of MurA when it is present in excess (30). Because the *murB* sequences of $Hungary^{19A}$ and D39 differ, we tested whether *murB* switch mutants of strains D39 (GenBank accession no. ABJ54032.1) and $Hungary^{19A}$ (ACA35854.1) exhibited any altered behavior in fosfomycin PAPs. This was not the case, as mutants carrying *murA1* and *murB* from the strain with the opposite fosfomycin heteroresistance phenotype behaved as is characteristic of their respective backgrounds (Fig. 4D).

Our results indicate that MurA1 is required for heteroresistance to fosfomycin, but there is another factor within the genome that determines the heteroresistance phenotype. This conclusion is consistent with the findings of studies investigating the mechanism of heteroresistance to methicillin in staphylococci which identified a gene crucial to the heteroresistance phenotype but also proposed a role for an unknown factor X (13, 14) or *chr** (15).

Here we have shown that heteroresistance to fosfomycin is the predominant phenotype of *S. pneumoniae*. We found that heteroresistance to fosfomycin can occur in the absence of heteroresistance to penicillin and *vice versa*, suggesting that different mechanisms cause heteroresistance to different antimicrobial agents.

Appreciation of the existence of heteroresistance of *S. pneumoniae* to antibiotics and understanding of the mechanisms by which it arises are important, as the phenomenon might represent a mechanism of bacterial survival of therapeutic concentrations of a given antibiotic resulting in clinical treatment failure. The predominance of heteroresistance to fosfomycin

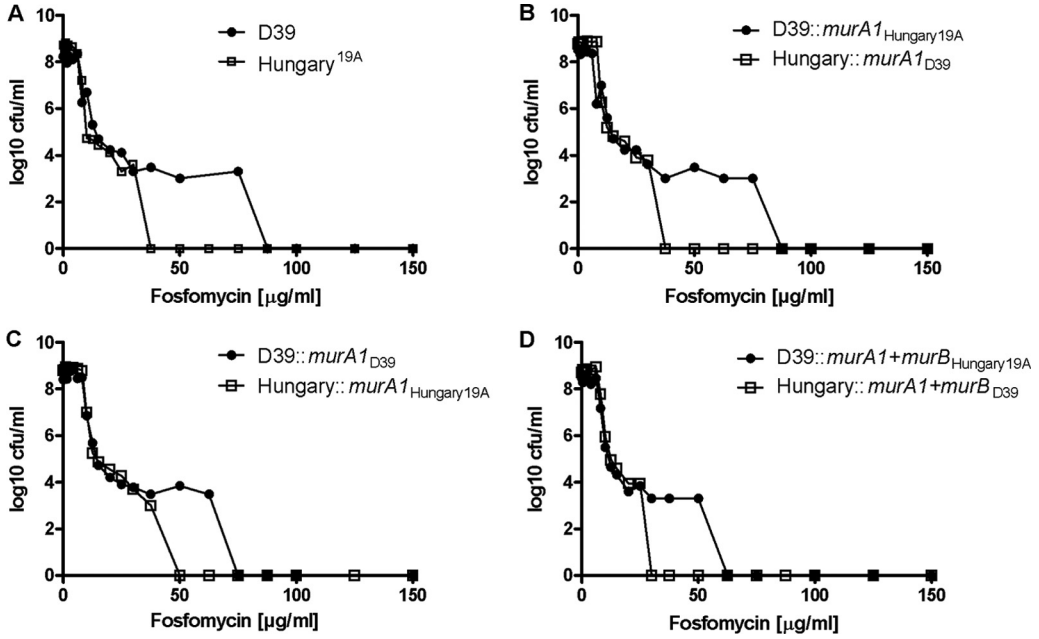

FIG 4 PAPs of D39 and Hungary19A wild-type strains, *murA1* switch mutants, *murA1* and *murB* switch mutants, and back transformants. Representative values of triplicate experiments are shown. (A) D39 compared to $Hungary^{19A}$ wild-type strain. (B) D39 switch mutant containing *murA1* of $Hungary^{19A}$ and vice versa. (C) Back transformants containing the spectinomycin resistance cassette of the *murA1* switch mutants. (D) Mutants containing switched *murA1* and *murB* genes.

described here may influence decisions on the use of this antibiotic against pneumococcal infections in the future.

ACKNOWLEDGMENTS

We thank Suzanne Aebi and Marianne Küffer for excellent technical assistance and SLS staff for help in X-ray data collection. We also thank J. K. Trczinski (Harvard School of Public Health, Boston, MA) for the Janus cassette, Andrew Camilli (Tufts University, Boston, MA) for the pR412 plasmid, J. Frey (Institute of Veterinary Bacteriology, University of Bern, Bern, Switzerland) for the *E. coli* SURE and BL21 strains, Dalia Denapaite (Technical University of Kaiserslautern, Kaiserslautern, Germany) for advice on genetic constructions, and Andrea Endimiani for critical reading of the manuscript.

This study was supported by grants from the Spanish Ministry of Economy and Competitiveness (BFU2011-25326), the Madrid Regional Government (S2010/BMD-2457), and the Swiss Centre for Antibiotic Resistance (www.anresis.ch).

REFERENCES

1. **Hakenbeck R, Grebe T, Zahner D, Stock JB.** 1999. β-Lactam resistance in *Streptococcus pneumoniae*: penicillin-binding proteins and non-penicillin-binding proteins. Mol. Microbiol. **33**:673–678.
2. **Contreras-Martel C, Dahout-Gonzalez C, Martins Ados S, Kotnik M, Dessen A.** 2009. PBP active site flexibility as the key mechanism for β-lactam resistance in pneumococci. J. Mol. Biol. **387**:899–909.
3. **Zerfass I, Hakenbeck R, Denapaite D.** 2009. An important site in PBP2x of penicillin-resistant clinical isolates of *Streptococcus pneumoniae*: mutational analysis of Thr338. Antimicrob. Agents Chemother. **53**:1107–1115.
4. **Morand B, Mühlemann K.** 2007. Heteroresistance to penicillin in *Streptococcus pneumoniae*. Proc. Natl. Acad. Sci. U. S. A. **104**:14098–14103.
5. **Falagas ME, Makris GC, Dimopoulos G, Matthaiou DK.** 2008. Heteroresistance: a concern of increasing clinical significance? Clin. Microbiol. Infect. **14**:101–104.
6. **Alam MR, Donabedian S, Brown W, Gordon J, Chow JW, Zervos MJ, Hershberger E.** 2001. Heteroresistance to vancomycin in *Enterococcus faecium*. J. Clin. Microbiol. **39**:3379–3381.
7. **Hung KH, Wang MC, Huang AH, Yan JJ, Wu JJ.** 2012. Heteroresistance to cephalosporins and penicillins in *Acinetobacter baumannii*. J. Clin. Microbiol. **50**:721–726.
8. **Li J, Rayner CR, Nation RL, Owen RJ, Spelman D, Tan KE, Liolios L.** 2006. Heteroresistance to colistin in multidrug-resistant *Acinetobacter baumannii*. Antimicrob. Agents Chemother. **50**:2946–2950.
9. **Rinder H, Mieskes KT, Loscher T.** 2001. Heteroresistance in *Mycobacterium tuberculosis*. Int. J. Tuberc. Lung Dis. **5**:339–345.
10. **de Lencastre H, Tomasz A.** 1994. Reassessment of the number of auxiliary genes essential for expression of high-level methicillin resistance in *Staphylococcus aureus*. Antimicrob. Agents Chemother. **38**:2590–2598.
11. **Ender M, Berger-Bächi B, McCallum N.** 2009. A novel DNA-binding protein modulating methicillin resistance in *Staphylococcus aureus*. BMC Microbiol. **9**:15. doi:10.1186/1471-2180-9-15.
12. **Finan JE, Rosato AE, Dickinson TM, Ko D, Archer GL.** 2002. Conversion of oxacillin-resistant staphylococci from heterotypic to homotypic resistance expression. Antimicrob. Agents Chemother. **46**:24–30.
13. **Hartman BJ, Tomasz A.** 1986. Expression of methicillin resistance in heterogeneous strains of *Staphylococcus aureus*. Antimicrob. Agents Chemother. **29**:85–92.
14. **Murakami K, Tomasz A.** 1989. Involvement of multiple genetic determinants in high-level methicillin resistance in *Staphylococcus aureus*. J. Bacteriol. **171**:874–879.
15. **Ryffel C, Strassle A, Kayser FH, Berger-Bächi B.** 1994. Mechanisms of heteroresistance in methicillin-resistant *Staphylococcus aureus*. Antimicrob. Agents Chemother. **38**:724–728.
16. **Tomasz A, Nachman S, Leaf H.** 1991. Stable classes of phenotypic expression in methicillin-resistant clinical isolates of staphylococci. Antimicrob. Agents Chemother. **35**:124–129.
17. **Avery SV.** 2006. Microbial cell individuality and the underlying sources of heterogeneity. Nat. Rev. Microbiol. **4**:577–587.
18. **Perales A, Martínez-Ripoll M, Fayos J, von Carstenn-Lichterfelde C, Fernandez M.** 1982. The absolute configuration of active and inactive fosfomycin. Acta Crystallogr. B **38**:2763–2764.
19. **Michalopoulos AS, Livaditis IG, Gougoutas V.** 2011. The revival of fosfomycin. Int. J. Infect. Dis. **15**:e732–e739.
20. **Kikuchi K, Totsuka K, Shimizu K, Ishii T, Yoshida T, Orikasa Y.** 1995. Effects of combination of benzylpenicillin and fosfomycin on penicillin-resistant *Streptococcus pneumoniae*. Microb. Drug Resist. **1**:185–189.
21. **Miró JM, Entenza JM, Del Rio A, Velasco M, Castaneda X, Garcia de la Maria C, Giddey M, Armero Y, Pericas JM, Cervera C, Mestres CA, Almela M, Falces C, Marco F, Moreillon P, Moreno A.** 2012. High-dose daptomycin plus fosfomycin is safe and effective in treating methicillin-susceptible and methicillin-resistant *Staphylococcus aureus* endocarditis. Antimicrob. Agents Chemother. **56**:4511–4515.
22. **Gunetileke KG, Anwar RA.** 1968. Biosynthesis of uridine diphospho-*N*-acetylmuramic acid. II. Purification and properties of pyruvate-uridine diphospho-*N*-acetylglucosamine transferase and characterization of uridine diphospho-*N*-acetylenopyruvylglucosamine. J. Biol. Chem. **243**:5770–5778.
23. **Walsh CT, Benson TE, Kim DH, Lees WJ.** 1996. The versatility of phosphoenolpyruvate and its vinyl ether products in biosynthesis. Chem. Biol. **3**:83–91.
24. **Du W, Brown JR, Sylvester DR, Huang J, Chalker AF, So CY, Holmes DJ, Payne DJ, Wallis NG.** 2000. Two active forms of UDP-*N*-acetylglucosamine enolpyruvyl transferase in gram-positive bacteria. J. Bacteriol. **182**:4146–4152.
25. **Wanke C, Amrhein N.** 1993. Evidence that the reaction of the UDP-*N*-acetylglucosamine 1-carboxyvinyltransferase proceeds through the O-phosphothioketal of pyruvic acid bound to Cys115 of the enzyme. Eur. J. Biochem. **218**:861–870.
26. **Marquardt JL, Brown ED, Lane WS, Haley TM, Ichikawa Y, Wong CH, Walsh CT.** 1994. Kinetics, stoichiometry, and identification of the reactive thiolate in the inactivation of UDP-GlcNAc enolpyruvoyl transferase by the antibiotic fosfomycin. Biochemistry **33**:10646–10651.
27. **Kim DH, Lees WJ, Walsh CT.** 1995. Stereochemical analysis of the tetrahedral adduct formed at the active site of UDP-GlcNAc enolpyruvyl transferase from the pseudosubstrates, (*E*)- and (*Z*)-3-fluorophosphoenolpyruvate, in D2O. J. Am. Chem. Soc. **117**:6380–6381.
28. **Han H, Yang Y, Olesen SH, Becker A, Betzi S, Schonbrunn E.** 2010. The fungal product terreic acid is a covalent inhibitor of the bacterial cell wall biosynthetic enzyme UDP-*N*-acetylglucosamine 1-carboxyvinyltransferase (MurA). Biochemistry **49**:4276–4282.
29. **Eschenburg S, Kabsch W, Healy ML, Schonbrunn E.** 2003. A new view of the mechanisms of UDP-*N*-acetylglucosamine enolpyruvyl transferase (MurA) and 5-enolpyruvylshikimate-3-phosphate synthase (AroA) derived from X-ray structures of their tetrahedral reaction intermediate states. J. Biol. Chem. **278**:49215–49222.
30. **Zhu JY, Yang Y, Han H, Betzi S, Olesen SH, Marsilio F, Schonbrunn E.** 2012. Functional consequence of covalent reaction of phosphoenolpyruvate with UDP-*N*-acetylglucosamine 1-carboxyvinyltransferase (MurA). J. Biol. Chem. **287**:12657–12667.
31. **Schönbrunn E, Sack S, Eschenburg S, Perrakis A, Krekel F, Amrhein N, Mandelkow E.** 1996. Crystal structure of UDP-*N*-acetylglucosamine enolpyruvyltransferase, the target of the antibiotic fosfomycin. Structure **4**:1065–1075.
32. **Skarzynski T, Mistry A, Wonacott A, Hutchinson SE, Kelly VA, Duncan K.** 1996. Structure of UDP-*N*-acetylglucosamine enolpyruvyl transferase, an enzyme essential for the synthesis of bacterial peptidoglycan, complexed with substrate UDP-*N*-acetylglucosamine and the drug fosfomycin. Structure **4**:1465–1474.
33. **Sung CK, Li H, Claverys JP, Morrison DA.** 2001. An *rpsL* cassette, Janus, for gene replacement through negative selection in *Streptococcus pneumoniae*. Appl. Environ. Microbiol. **67**:5190–5196.
34. **Meier PS, Utz S, Aebi S, Mühlemann K.** 2003. Low-level resistance to rifampin in *Streptococcus pneumoniae*. Antimicrob. Agents Chemother. **47**:863–868.
35. **Shevchuk NA, Bryksin AV, Nusinovich YA, Cabello FC, Sutherland M, Ladisch S.** 2004. Construction of long DNA molecules using long PCR-based fusion of several fragments simultaneously. Nucleic Acids Res. **32**:e19. doi:10.1093/nar/gnh014.
36. **Brugger SD, Hathaway LJ, Mühlemann K.** 2009. Detection of *Streptococcus pneumoniae* strain cocolonization in the nasopharynx. J. Clin. Microbiol. **47**:1750–1756.
37. **Hathaway LJ, Battig P, Mühlemann K.** 2007. In vitro expression of the first capsule gene of *Streptococcus pneumoniae*, *cpsA*, is associated with

serotype-specific colonization prevalence and invasiveness. Microbiology **153**:2465–2471.
38. **Matthews BW.** 1968. Solvent content of protein crystals. J. Mol. Biol. **33**:491–497.
39. **Kabsch W.** 2010. XDS. Acta Crystallogr. D Biol. Crystallogr. **66**:125–132.
40. **Evans P.** 2006. Scaling and assessment of data quality. Acta Crystallogr. D. Biol. Crystallogr. **62**:72–82.
41. **Winn MD, Ballard CC, Cowtan KD, Dodson EJ, Emsley P, Evans PR, Keegan RM, Krissinel EB, Leslie AG, McCoy A, McNicholas SJ, Murshudov GN, Pannu NS, Potterton EA, Powell HR, Read RJ, Vagin A, Wilson KS.** 2011. Overview of the CCP4 suite and current developments. Acta Crystallogr. D Biol. Crystallogr. **67**:235–242.
42. **McCoy AJ, Grosse-Kunstleve RW, Adams PD, Winn MD, Storoni LC, Read RJ.** 2007. Phaser crystallographic software. J. Appl. Crystallogr. **40**: 658–674.
43. **Adams PD, Afonine PV, Bunkoczi G, Chen VB, Davies IW, Echols N, Headd JJ, Hung LW, Kapral GJ, Grosse-Kunstleve RW, McCoy AJ, Moriarty NW, Oeffner R, Read RJ, Richardson DC, Richardson JS, Terwilliger TC, Zwart PH.** 2010. PHENIX: a comprehensive Python-based system for macromolecular structure solution. Acta Crystallogr. D Biol. Crystallogr. **66**:213–221.
44. **Emsley P, Lohkamp B, Scott WG, Cowtan K.** 2010. Features and development of Coot. Acta Crystallogr. D Biol. Crystallogr. **66**:486–501.
45. **Chen VB, Arendall WB, III, Headd JJ, Keedy DA, Immormino RM, Kapral GJ, Murray LW, Richardson JS, Richardson DC.** 2010. MolProbity: all-atom structure validation for macromolecular crystallography. Acta Crystallogr. D Biol. Crystallogr. **66**:12–21.
46. **Schönbrunn E, Eschenburg S, Krekel F, Luger K, Amrhein N.** 2000. Role of the loop containing residue 115 in the induced-fit mechanism of the bacterial cell wall biosynthetic enzyme MurA. Biochemistry **39**:2164–2173.
47. **Meroueh SO, Roblin P, Golemi D, Maveyraud L, Vakulenko SB, Zhang Y, Samama JP, Mobashery S.** 2002. Molecular dynamics at the root of expansion of function in the M69L inhibitor-resistant TEM β-lactamase from *Escherichia coli*. J. Am. Chem. Soc. **124**:9422–9430.
48. **Hauser C, Aebi S, Mühlemann K.** 2004. An internationally spread clone of *Streptococcus pneumoniae* evolves from low-level to higher-level penicillin resistance by uptake of penicillin-binding protein gene fragments from nonencapsulated pneumococci. Antimicrob. Agents Chemother. **48**: 3563–3566.
49. **Hathaway LJ, Stutzmann Meier P, Battig P, Aebi S, Mühlemann K.** 2004. A homologue of *aliB* is found in the capsule region of nonencapsulated *Streptococcus pneumoniae*. J. Bacteriol. **186**:3721–3729.
50. **Bättig P, Mühlemann K.** 2007. Capsule genes of *Streptococcus pneumoniae* influence growth in vitro. FEMS Immunol. Med. Microbiol. **50**: 324–329.